0026-895X/96/061541-10$3.00/0

MOLECULAR PHARMACOLOGY, 50:1541–1550 (1996).

Subtype-Selective Inhibition of *N*-Methyl-D-aspartate Receptors by Haloperidol

V. I. ILYIN,[1] E. R. WHITTEMORE, J. GUASTELLA, E. WEBER, and R. M. WOODWARD

Acea Pharmaceuticals (a subsidiary of CoCensys Inc.) Irvine, California 92618

Received March 25, 1996; Accepted August 12, 1996

SUMMARY

Previous studies indicate that haloperidol, a therapeutically useful antipsychotic drug, inhibits neuronal *N*-methyl-D-aspartate (NMDA) responses and has neuroprotective effects against NMDA-induced brain injury. To further characterize this inhibition, we used electrical recordings to assay the effects of haloperidol on four diheteromeric subunit combinations of cloned rat NMDA receptors expressed in *Xenopus laevis* oocytes: NR1A coexpressed with NR2A, NR2B, NR2C, or NR2D. Haloperidol selectively blocks NR1A/2B subunit combinations (IC_{50} = ~3 μM; maximum inhibition, ~85%), whereas the other subunit combinations are ≥100-fold less sensitive (IC_{50} = >300 μM). Inhibition of NR1A/2B receptors is insurmountable with respect to glutamate and glycine and does not exhibit voltage dependence. The splice variant combinations NR1B/2B and NR1e/2B are also blocked by haloperidol. In oocytes from some frogs, 30–100 μM haloperidol induces potentiation of NR1A/2A receptor responses. NMDA responses in E16-17 rat cortical neurons cultured for ≤10 days are inhibited by haloperidol at the same potency and to the extent as NR1/2B receptors (IC_{50} = ~2 μM; maximum inhibition, ~80%). In contrast, cells cultured for longer periods show a wide range of sensitivity. This change in pharmacology coincides with a developmental switch in subunit expression; from NR1 expressed with NR2B to NR1 coexpressed with NR2A and NR2B. Inhibition of macroscopic neuronal NMDA responses is mechanistically similar to inhibition of NR1A/2B receptors. Single-channel recordings from neurons show that antagonism is associated with a decrease in the frequency of channel openings and a shortening of mean channel open time. Collectively, our experiments indicate that haloperidol selectively inhibits NMDA receptors comprised of NR1 and NR2B subunits. Inhibition is consistent with action at a noncompetitive allosteric site that is distinct from the glutamate-, glycine-, and phencyclidine-binding sites and is probably mechanistically related to the atypical antagonist ifenprodil. Our results suggest that haloperidol can be used as a tool for investigating NMDA receptor subunit composition and can serve as a structural lead for designing novel subtype-selective NMDA receptor ligands.

Mammalian NMDA receptors are ligand-gated ion channels comprised of hetero-oligomeric assemblies of polypeptide subunits (1). The majority of neuronal NMDA receptors are thought to contain at least two types of subunit assembled into diheteromeric or triheteromeric combinations (1–5). The rat subunits have been designated NR1 and NR2. At present, one gene has been found encoding the NR1 subunit, and four genes have been found encoding NR2 subunits; these are called NR2A–2D (3, 4, 6). The NR1 subunit is found in seven different isoforms that are generated by alternative RNA splicing (1, 2, 7). Different subunit combinations generate NMDA receptors with different biophysical and pharmacological properties (1–4, 7–10). In addition, *in situ* hybridization studies suggest that the NR1 splice variants and the four NR2 subunits have distinct ontology and patterns of expression in the rat central nervous system (3–7). The complexity of NMDA receptor molecular biology implies that there are multiple subtypes of NMDA receptor in mammalian brain. Heterogeneity in NMDA receptor properties measured in different brain regions and changes in receptor properties during the course of development strongly support this idea (1, 11–13).

Numerous *in vitro* and *in vivo* studies indicate that NMDA receptors play an important role in mediating the excitotoxic effects of glutamate (14). In the simplest terms, prolonged exposure to glutamate causes excessive influx of Ca^{2+} through NMDA receptors, which initiates a pathological cascade that leads to cell death (14). NMDA receptor antagonists have therefore attracted considerable attention as potential therapeutic neuroprotectants that could help to minimize the brain damage induced by ischemic stroke and head trauma (15). In 1990, MacDonald and Johnston reported that haloperidol, a potent D_2 dopamine receptor antagonist and σ site ligand (16, 17), had neuroprotective effects against NMDA-induced brain injury (18). The mechanism of action was un-

[1] Permanent affiliation: Laboratory of Nerve Cell Biophysics, Institute of Cell Biophysics, Russian Academy of Sciences, Puschino, Moscow Region, 142292, Russia.

ABBREVIATIONS: NMDA, *N*-methyl-D-aspartate; AMPA, α-amino-3-hydroxy-5-methylisoxazole-4-propionic acid; HEPES, 4-(2-hydroxyethyl)-1-piperazineethanesulfonic acid; DMSO, dimethylsulfoxide; EGTA, ethylene glycol bis(β-aminoethyl ether)-*N*,*N*,*N*′,*N*′-tetraacetic acid.

certain. Subsequently, Fletcher and MacDonald (19) found that haloperidol was an antagonist of NMDA receptor responses in cultured rat hippocampal neurons. In these experiments, the mechanism of inhibition seemed to involve partial agonism/competitive antagonism at the NMDA receptor glycine site. It followed that the neuroprotective effects of haloperidol might be due to direct inhibition of NMDA receptors.

The idea that haloperidol inhibits NMDA receptors by interaction at the glycine site was intriguing because the drug has no obvious structural relationship with other known glycine-site ligands (20). We reasoned that haloperidol might serve as a lead compound for a completely novel structural class of glycine site antagonists. To begin to explore this possibility, we used electrophysiological assays to characterize the actions of haloperidol on cloned rat brain NMDA receptors expressed in *Xenopus laevis* oocytes (2, 3, 10, 21) and on NMDA receptors expressed by cultured rat cortical neurons (10). The current detailed study was prompted by experiments indicating that haloperidol shows strong subtype selectivity in its antagonism of NMDA receptors. Preliminary reports of this work have appeared in abstract form (for example, see ref. 22).

Materials and Methods

Preparation of RNA. cDNA clones encoding the NR1A, NR2A, NR2B, NR2C, and NR2D rat NMDA receptor subunits were provided by Dr. P. H. Seeburg (Heidelberg University, Heidelberg, Germany) (3, 6). cDNA clones encoding the NR1 splice variants NR1B and NR1e were provided by Dr. S. Nakanishi (Kyoto University, Kyoto, Japan) (21). For the splice variants, we adopted the terminology of Sugihara *et al.* (21) but use a small capital letter to indicate, that in contrast to NR2, these subunits originate from a single gene. In alternative nomenclature, the NR1A variant corresponds to $NR1_{011}$, NR1B to $NR1_{111}$, and NR1E to $NR1_{000}$ (7). All clones were prepared using conventional techniques, and cRNA was synthesized with T3 RNA polymerase. cRNA was diluted to 400 ng/μl and stored at −80°. Poly(A)$^+$ RNA from rat forebrain was prepared as described previously (10).

The *X. laevis* oocyte expression system. In general, preparation and microinjection of oocytes were as reported previously (10). Briefly, frogs were anesthetized (30–60 min) with 0.15% 3-aminobenzoic acid ethyl ester (MS-222). A small portion of the ovary was surgically removed, and mature oocytes were dissected still surrounded by their enveloping layers. The inner ovarian epithelium and most of the follicle cell layer were removed enzymatically by treatment with collagenase (0.5 mg/ml, 45–75 min; Boehringer-Mannheim Biochemicals, Indianapolis, IN). Oocytes were stored in Barth's medium containing 88 mM NaCl, 1 mM KCl, 0.41 mM $CaCl_2$, 0.33 mM $Ca(NO_3)_2$, 0.82 mM $MgSO_4$, 2.4 mM $NaHCO_3$, and 5 mM HEPES, pH 7.4, with 0.1 mg/ml gentamycin sulfate. On the following day, denuded oocytes were injected with 2–20 ng of NMDA receptor-encoding cRNAs (depending on expressional potency) or with ~50 ng of rat brain poly(A)$^+$ RNA. NR1A/NR2A was injected at a 1:1 or 1:4 ratio, depending on the expressional potency of the NR2A cRNA. All other binary subunit combinations were injected at 1:1. Electrical recordings were made using a Dagan TEV-200 voltage-clamp in a 0.1-ml recording chamber continuously perfused (5–10 ml/min) with frog Ringer's solution containing 115 mM NaCl, 2 mM KCl, 1.8 mM $CaCl_2$, and 5 mM HEPES, pH 7.4. Drugs were applied by bath perfusion. Zero-Ca^{2+}/Ba^{2+} Ringer's solution was composed of 115 mM NaCl, 2 mM KCl, 1.8 mM $BaCl_2$, and 5 mM HEPES, pH 7.4. Intraoocyte injection of the Ca^{2+}-chelating agents 1,2-bis(2-aminophenoxy)ethane-*N*,*N*,*N*′,*N*′-tetraacetic acid or EGTA (~100-500 pmol/cell) was by pressure ejection from micropipettes (10). The volume of injections was estimated by measuring droplet diameters in air before and after insertion of pipettes into oocytes.

Culture of rat cortical neurons. Primary cultures of mixed cortical neurons were obtained from Sprague-Dawley (Charles River, Hollistar, CA) rat embryos on embryonic day 16 or 17, using a modification of procedures described previously (23). Briefly, after dissection, cortices were incubated for 8–10 min in 0.25% trypsin/0.5 mM EDTA at 37° in a Ca^{2+}/Mg^{2+}-free Hanks' balanced salt solution containing 138 mM NaCl, 5 mM KCl, 0.3 mM KH_2PO_4, 0.3 mM Na_2HPO_4, 5.6 mM D-glucose, 4.2 mM $NaHCO_3$, 1 mM pyruvate, and 20 mM HEPES. Trypsin digestion was terminated by washing with Neurobasal medium (GIBCO, Grand Island, NY) containing 10% fetal calf serum. Tissue was triturated and passed through a nylon mesh (Falcon Plastics, Oxnard, CA) to remove clumps of undissociated cells and debris. Culture dishes (Costar or Nunc 35 mm) were precoated with poly-D-lysine. Cells were plated at a density of 3–5 × 10^4/cm^2 in Neurobasal medium supplemented with 5% fetal calf serum, 0.5 mM L-glutamine, and 0.25 μM L-glutamate. Neurons were maintained at 37° in a humidified incubator (5% CO_2/95% air). After 4–5 days, the plating medium was replaced with Neurobasal medium supplemented with 5% fetal calf serum and 0.5 mM L-glutamine. Cultures were fed with this medium twice weekly and maintained for 3 days to 4 weeks.

Electrophysiology in cultured neurons. Whole-cell or single-channel currents were recorded using standard patch-clamp techniques (24). Drugs and intervening wash were applied from a microcapillary linear array (Microcaps, 2-μl volume; Drummond Scientific, Broomall, PA); this controlled the solution surrounding the cell under examination. The microcapillary array positioning was governed via remote control with a motorized drive (model 860; Newport, Fountain Valley, CA). The external solution for all drug applications and wash contained 150 mM NaCl, 4 mM KCl, 1 mM $CaCl_2$, 10 mM Na-HEPES, pH 7.4, and 400 nM tetrodotoxin, 310 mOsM. In addition, the recording chamber was continuously superfused (~5 ml/min) by the same solution supplemented with 2 mM $MgCl_2$ and 10 mM glucose. The internal pipette solution for whole-cell recordings contained 145 mM CsCl, 10 mM Cs-HEPES, pH 7.4, 0.5 mM $CaCl_2$, and 10 mM EGTA, with 2 mM ATP and 1 mM GTP, 290 mOsM. ATP and GTP were added fresh each day, and the solution was stored on ice. For excised patches, CsCl was replaced by equimolar CsF, and ATP and GTP were omitted from the solution. Recordings were made with an Axopatch 200A amplifier (Axon Instruments, Foster City, CA). Pipettes (6–10 MΩ) were pulled from thick-walled borosilicate capillaries with filament (World Precision Instruments, New Haven, CT), and were either non-fire-polished (whole cell) or fire-polished (excised patch). Whole-cell currents were filtered at 2 kHz via a four-pole, −3 dB, low-pass Bessel filter and stored digitally on a Nicolet-310 digital oscilloscope (Nicolet Instrument, Madison, WI). Recordings were analyzed off-line using software provided by the laboratory of Dr. Ricardo Miledi (University of California, Irvine). Single-channel currents were stored for later analysis on a digital tape recorder (DTC-59ES, Sony Corporation) modified to record direct-current signals.

Data analysis: pharmacology. Pharmacology of whole-cell currents was analyzed as reported previously (10). Briefly, data for glycine and glutamate concentration-response relations were fit using the logistic equation:

$$I/I_{max} = 1/\{1 + (EC_{50}/[agonist])^n\} \quad (1)$$

where I is the measured current, I_{max} is the maximum steady state current, n is the slope factor, and EC_{50} is the concentration of drug that elicits a half-maximal response (SigmaPlot; Jandel Scientific, San Rafael, CA). Concentration-inhibition curves for haloperidol were fit with eq. 2:

$$I/I_{control} = \min + \{(1 - \min)/[1 + ([antagonist]/IC_{50})^n]\} \quad (2)$$

where $I_{control}$ is the current in the absence of antagonist, min (minimum) is the residual fractional response at saturating concentration of antagonist, and IC_{50} is the concentration of drug that causes half of this level of inhibition. Values in the text are given as mean ± standard error. Values for p were calculated with Student's t tests or by one-way analysis of variance (Excel; Microsoft, Redmond, WA).

Data analysis: single-channel recording. Low concentrations of NMDA (4 μM) and glycine (500 nm) were used to minimize the number of overlapping events. Single-channel currents were replayed, filtered at 4 kHz (−3 dB, four-pole, low-pass Bessel; Frequency Devices, Haverhill, MA), digitized at 10 kHz, and analyzed on an IBM PC-compatible computer using pClamp6 software (Axon Instruments). Sampling was done using a DigiData 1200 interface (Axon Instruments). Single-channel data were collected in 30–90-sec blocks. To plot distributions of dwell times, openings and closings were defined using a 50% threshold criterion (25). Events briefer than twice the system rise time (~180 μsec) were ignored. Amplitude histograms were fit to the sum of one or more gaussian functions using the least-squares curve-fitting routine in PSTAT. Subconductance states were not analyzed (main conductance level, ~48 pS). Open-time histograms were best fit with the sum of two exponentials. Because multichannel patches were used, an overall estimate of mean channel open time (t_o) was calculated by applying eq. 3:

$$t_o = \left(\sum j t_j\right)/N \qquad (3)$$

where j is the current level, t_j is the dwell time at current level j (over the whole record), and N is the total number of channel openings (26). For the same reason, the estimate of opening probability (P) was nP, where n is the number of channels and P is the probability of opening for a single-channel.

Drugs. Haloperidol was obtained from Research Biochemicals (Natick, MA). Other drugs were from Sigma Chemical (St. Louis, MO) or GIBCO. Haloperidol was initially made up in a series of DMSO stocks over the range of 0.01–100 mM. Ringer's solutions (0.01–100 μm) were made with 300 to 3000-fold dilution of stocks. At these concentrations, DMSO had little or no effect on steady state membrane current responses.

Results

Cloned NMDA Receptors Expressed in *X. laevis* Oocytes

Subunit-selective inhibition of cloned NMDA receptors. Effects of haloperidol on cloned NMDA receptors were measured using fixed saturating or near-saturating concentrations of agonists: NR1A/2A, 10 μM glycine/100 μM glutamate; and NR1A/2B, NR1A/2C, and NR1A/2D, 1 μM glycine/100 μM glutamate (Fig. 1). In normal Ringer's solution, coapplication of glutamate and glycine elicited the characteristic multiphasic NMDA response (Fig. 1) (9, 10). Antagonist potency was assessed from reductions in amplitude of the second phase (Fig. 1, *arrow*). Oocytes were pretreated with haloperidol and glycine, and the receptors were activated by the coapplication of glutamate.

Haloperidol was a highly selective inhibitor for NR1A/2B subunit combinations compared with NR1A/2A, NR1A/2C, and NR1A/2D (Fig. 1 and Table 1). At concentrations of ≤10 μM, haloperidol inhibition of NR1A/2B receptors fully reversed after a 5–10-min wash. At concentrations of >10 μM, inhibition washed out more slowly and was increasingly difficult to completely reverse (Fig. 1). Although haloperidol has limited solubility in saline (~100 μM with 0.1% DMSO), inhibition of NR1A/2B responses seemed to be incomplete, equilibrating at a maximum of 70–85%. Inhibition measured in Ba^{2+} Ringer's solution was similar to that measured in

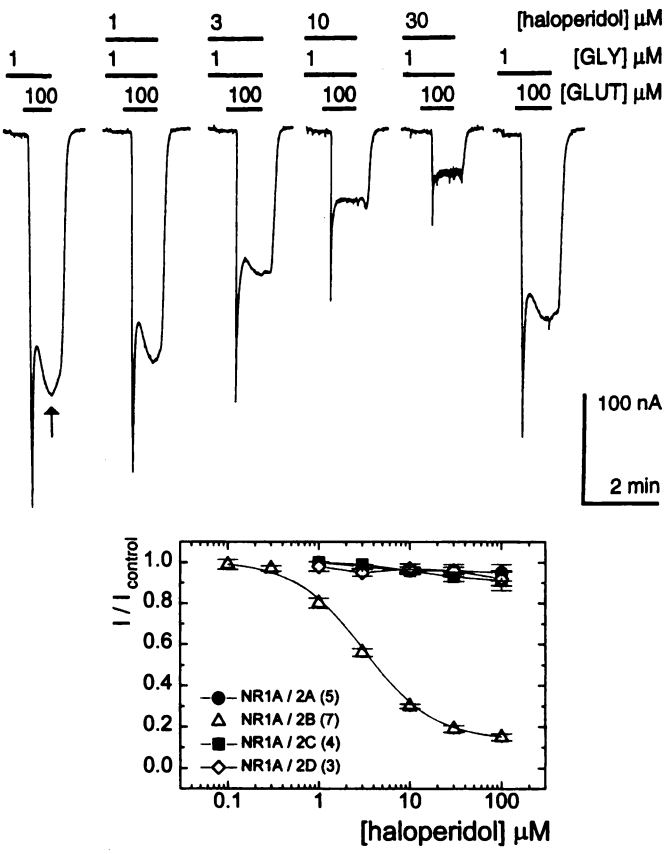

Fig. 1. *Top*, sample records illustrating inhibition of NMDA responses by haloperidol in an oocyte expressing NR1A/2B subunit combinations. Response amplitudes for pharmacological assays were measured on the second, or plateau, phase of the response (*arrow*). *Bars*, drug application. Dead time of the perfusion system was ~5 sec. To minimize rundown, responses were separated by 5–10-min intervals of wash. The holding potential was −70 mV. Inward current denoted by *downward deflection*. *Bottom*, concentration-inhibition curves for haloperidol showing effect of varying the NR2 subunit on haloperidol sensitivity. Data are mean ± standard error. Response amplitudes are expressed as a fraction of control values: 10 μM glycine and 100 μM glutamate for NR1A/2A, and 1 μM glycine and 100 μM glutamate for all other subunit combinations. *Smooth curve*, best fit of eq. 2 to the data. Curve parameters are given in Table 1. Current ranges and mean responses were NR1A/2A, 29–150 nA (73 ± 30 nA); NR1A/2B, 70–500 nA (200 ± 60 nA); NR1A/2C, 58–147 nA (99 ± 23 nA); and NR1A/2D, 52–61 nA (58 ± 4 nA); the oocytes were from six different frogs.

normal Ringer's. This indicates that any Cl^- current activated during the second phase of the response does not distort measurement of potency (9, 10). The IC_{50} value for haloperidol on NR1A/2B responses was typically ~3 μM. Subsequent experiments, however, using oocytes from a number of different frogs showed that IC_{50} values could vary by ≤3-fold: from ~3 μM to as high as 10 μM in occasional cells. The variability occurred between oocytes taken from different frogs and also between oocytes taken at the same time from the same ovary.

In oocytes expressing NR1A/2B subunits, 1 nM to 100 μM haloperidol neither activated current when applied alone nor increased the small currents elicited by glycine or glutamate when applied separately, currents that are probably due to trace contamination by the respective coagonist. At a holding potential of −70 mV, 10–100 μM haloperidol applied alone sometimes caused an "apparent" inward current, but this was associated with a decrease in membrane conductance

TABLE 1

Inhibition of NMDA responses by haloperidol

IC_{50} and slope values are the best fits of data to eq. 2. Inhibition of NMDA response was measured using saturating or near-saturating concentrations of agonists. Oocytes: NR1A alone, NR1A/2A, and NR1A/2A/2B, 10 μM glycine and 100 μM glutamate; NR1A/2B-D, 1 μM glycine and 100 μM glutamate. Neurons: 3 or 10 μM glycine and 100 μM NMDA (neurons ≤ 10 days *in vitro*). AMPA responses were activated with 10 μM AMPA in both preparations. Oocyte assays were in cells expressing rat cerebral cortex poly $(A)^+$ RNA. Current ranges and mean responses for the oocyte AMPA assays were 42 to 77 nA (64 ± 15 nA) (four experiments); values for neuronal AMPA assays were 70 to 328 pA (185 ± 107 nA) (four experiments). *n* indicates the number of independent experiments; numbers in parentheses are 95% confidence intervals.

Receptor/subunit	IC_{50}	Slope	Concentration-inhibition curve	Inhibition at 100 μM	*n*
	μM			%	
Oocyte recordings					
NR1A	~100			38 ± 3	4
NR1A/2A	>300			5 ± 4	5
NR1A/2B	3.1 (2.7–3.6)	−1.1	(−1.2, −1.0)	85 ± 2	7
NR1A/2C	>300			9 ± 5	4
NR1A/2D	>300			8 ± 4	3
NR1A/2B[a]	4.3 (2.8–6.8)	−0.9	(−1.1, −0.8)	80 ± 6	6
NR1B/2B[a]	5.1 (4.5–5.7)	−1.3	(−1.4, −1.2)	86 ± 2	5
NR1E/2B[a]	4.7 (3.6–6.3)	−1.1	(−1.2, −1.0)	78 ± 3	5
AMPA (rat brain)	>300			1.8 ± 1.7	4
Neuron recordings					
NMDA	1.8 (1.5–2.1)	−1.0	(−1.1, −0.9)	80 ± 2	25
AMPA	>300			2 ± 2	4

[a] Experiments using different batch of oocytes than those above.

(not shown). The effect was larger at more positive holding potentials and was probably due to blockade of endogenous K^+ channels. For other subunit combinations, the effects of haloperidol on responses elicited by nonsaturating concentrations of agonists were not tested.

To investigate the contribution of NR1 subunits to haloperidol sensitivity, we tested two additional splice variants, NR1B and NR1E, coexpressed with NR2B. NR1B/2B and NR1E/2B receptors showed similar sensitivity to haloperidol as NR1A/2B in assays in the same batch of oocytes (Table 1).

In addition, haloperidol was tested for antagonism of putative homomeric NR1A receptors and rat brain AMPA receptors expressed in oocytes. Responses in oocytes expressing NR1A subunits were generally <15 nA [i.e., ≤10% of responses seen with the diheteromeric subunit combinations (3, 4, 21)]. Partial inhibition curves showed that high concentrations of haloperidol caused ~40% block of these currents (Table 1). Putative homo-oligomeric receptors comprised of other NR1 splice variants were not tested for haloperidol sensitivity. Rat brain AMPA receptors were insensitive to inhibition by haloperidol (Table 1).

Potentiation of NR1/2A receptors. In subsequent experiments, we also found that 30–100 μM haloperidol would sometimes induce significant potentiation of NR1A/2A receptor responses. For example, in cells from one batch of oocytes, NR1A/2A receptor responses were increased 74 ± 21% by 100 μM haloperidol ($p < 0.05$). The threshold for this effect was ~10 μM haloperidol. In the same batch of oocytes, NR1A/2B receptors were inhibited by haloperidol at normal potency (IC_{50} = 2.6 ± 0.17 μM; maximum inhibition, 82 ± 1%; four experiments), whereas NR1A/2C and NR1A/2D receptors were unaffected. The potentiating effect of haloperidol on NR1A/2A receptors was fully reversible, washing out within 1–3 min. Measured in the same cell, levels of potentiation were comparable between recordings made in normal and Ba^{2+} Ringer's solution, indicating that the effect was not due to an increase in secondary Cl^- current (9, 10). Potentiation of NR1A/2A receptor responses varied among batches of oocytes, was seen only at high concentrations of haloperidol, and was not further studied.

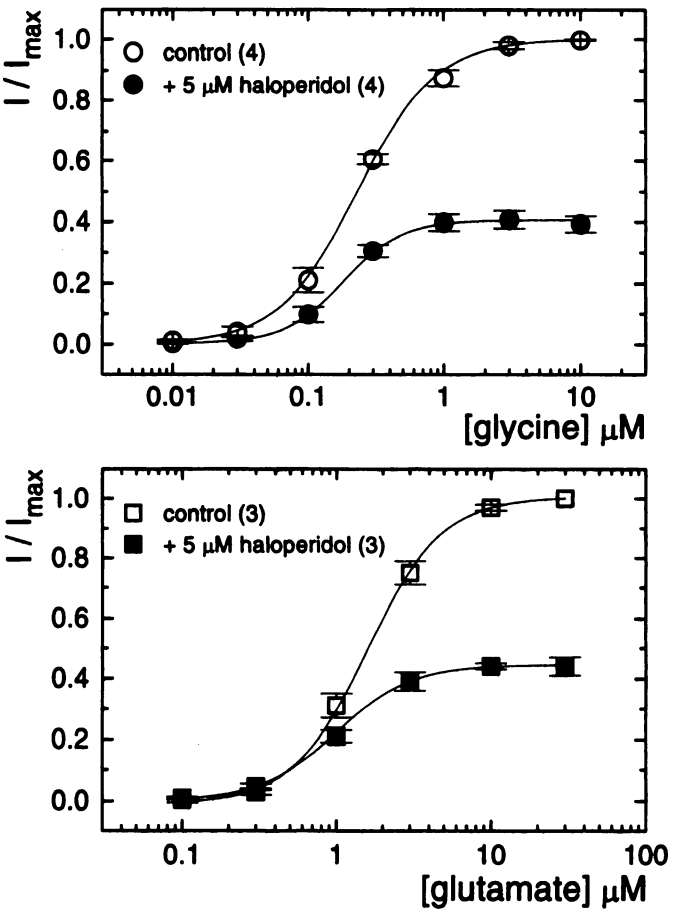

Fig. 2. Effect of haloperidol on concentration-response curves for glycine and glutamate in oocytes expressing NR1A/2B subunit combinations. *Top*, glycine concentration-response curve with glutamate fixed at 100 μM. *Bottom*, glutamate concentration-response curve with glycine fixed at 10 μM. Response amplitudes are expressed as a fraction of maximum currents. Data are presented as in legend to Fig. 1. *Smooth curves*, best fits of eq. 1 to the data. Curve parameters are given in Table 2. Current ranges and mean steady state responses were 88–185 nA (140 ± 20 nA) for glycine curves and 97–175 nA (130 ± 70 nA) for glutamate curves. Data are mean ± standard error.

TABLE 2

Effect of haloperidol on glycine and glutamate concentration-response curves

EC_{50} and slope values are the best fits of pooled data to eq. 1. For NR1A/2B, glycine curves were measured using 100 μM glutamate, and glutamate curves were measured using 10 μM glycine. For neuron recordings, glycine curves were measured using 100 μM NMDA, and NMDA curves were measured using 10 μM glycine.

NR1a/2B	EC_{50}	Slope	*n*
	μM		
Oocyte recordings:			
Glycine (control)	0.23 (0.22–0.26)	1.5 (1.3–1.7)	4
Glycine + 5 μM haloperidol	0.18 (0.17–0.20)	2.0 (1.7–2.3)	4
Glutamate (control)	1.6 (1.5–1.7)	1.8 (1.7–1.9)	3
Glutamate + 5 μM haloperidol	1.0 (0.9–1.1)	1.8 (1.6–2.0)	3
Neuron recordings:			
≤10 days *in vitro*			
Glycine (control)	0.079 (0.068–0.093)	1.2 (1.0–1.4)	5
Glycine + 4 μM haloperidol	0.28 (0.23–0.35)	1.4 (1.1–1.8)	3
NMDA (control)	26 (20–32)	1.0 (0.8–1.4)	7
NMDA + 4 μM haloperidol	17 (13–21)	1.1 (0.8–1.4)	5

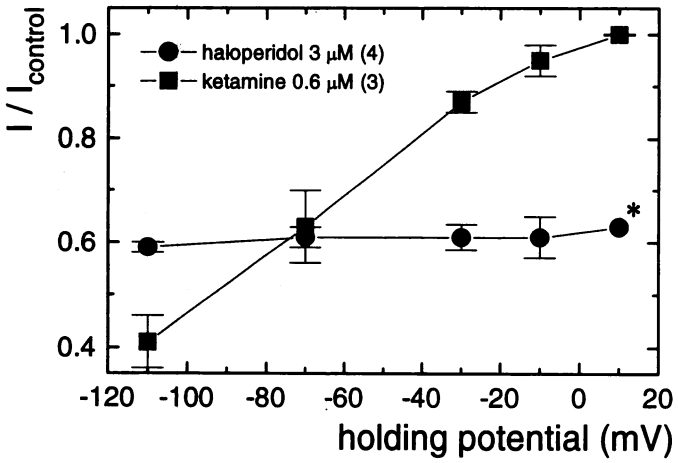

Fig. 3. Effect of voltage on inhibition by haloperidol and ketamine of NR1A/2B responses expressed in oocytes. Levels of inhibition were measured on currents elicited by saturating concentrations of agonists (10 μM glycine and 100 μM glutamate) and are presented as fractional responses. For these experiments, recordings were made in the zero-Ca^{2+}/Ba^{2+} Ringer's solution, and oocytes were injected with ~200 pmol of 1,2-bis(2-aminophenoxy)ethane-*N*,*N*,*N*′,*N*′-tetraacetic acid. Ketamine (0.6 μM) was selected to give similar inhibition at −70 mV as 3 μM haloperidol. *, Only one value at this voltage. Data are mean ± standard error.

Mechanism of NR1A/2B receptor antagonism. The mechanism of NR1A/2B receptor inhibition was investigated first by measuring the effects of a fixed concentration of haloperidol on the concentration-response curves for glycine and glutamate (Fig. 2). Antagonism induced by 5 μM haloperidol was not surmounted by increasing either glycine or glutamate concentrations (Fig. 2). In these experiments, inhibition was associated with a 22% increase in affinity for glycine ($p < 0.01$) and a 38% increase in affinity for glutamate ($p < 0.03$) (Table 2). Responses elicited by 0.3 μM glutamate were increased 50% by 5 μM haloperidol, whereas responses elicited by 30 μM glutamate were inhibited by 56%.

To test whether antagonism of NR1A/2B responses by haloperidol showed voltage dependence, levels of inhibition were measured at different holding potentials. For comparison, voltage dependence of inhibition was also assayed for ketamine, a well-characterized channel blocker and phencyclidine-site ligand (27). Over the range of −110 to +10 mV, antagonism by 3 μM haloperidol was independent of voltage (Fig. 3). In contrast, antagonism by 0.6 μM ketamine was characterized by pronounced voltage dependence over this range. Testing haloperidol at more positive voltages was difficult in oocytes due to activation of large endogenous currents (28), so these studies were done in neurons (see below).

Whole-Cell Patch-Clamp Recordings from Cultured Cortical Neurons

Haloperidol concentration-inhibition curves for neuronal NMDA responses. As described previously (19, 29), NMDA responses in cultured rat cortical neurons were inward currents at −60 mV, consisting of a rapid rising phase followed by desensitization to a steady state level (see Fig. 5). In an effort to standardize experiments, recordings were made from neurons with large cell bodies and a "pyramidal-like" morphology (23). With saturating concentrations of agonists, peak amplitudes of current increased with duration of culture, ranging from an average of 471 ± 58 pA at 3–5 days (31 cells in eight cultures) to 1154 ± 101 pA after 2–3 weeks *in vitro* (32 cells in seven cultures). These values may underestimate peak amplitudes because the speed of drug application was limited by the linear array system. In the same sample of cells, currents measured at the plateau phase increased 5-fold, from 156 ± 18 to 805 ± 76 pA. As the cultures aged, the measured levels of desensitization became less pronounced. In young cultures, the steady state-to-peak ratio was 0.35 ± 0.03, whereas in older cultures, the ratio was 0.72 ± 0.03. Again, accuracy of these values was probably compromised by the speed of drug application. Level of response run-down varied between cells and was most pronounced over the first 5–10 min of recording. All inhibition curves were assayed under steady state desensitizing conditions on the plateau phase of the response.

As reported for cultured hippocampal neurons (19), initial experiments indicated that haloperidol had variable effects on NMDA responses in cultured cortical neurons. Responses in some neurons were inhibited at approximately the same potency and to the same degree as NR1A/2B receptors expressed in oocytes. In other neurons, NMDA responses were unaffected by haloperidol at concentrations ≤100 μM. In some cells, peak currents were increased by the higher concentrations of haloperidol (19). With further experiments, a pattern became evident. In young cultures, NMDA responses in the majority of cells were robustly inhibited by haloperidol. In older cultures, responses showed variable sensitivity; this is illustrated in Fig. 4, in which the embryonic day 16–17 neurons have been divided into two groups: ≤10 days and >10 days *in vitro*. For neurons ≤10 days *in vitro*, NMDA responses in 89% of the 28 cells examined were blocked by haloperidol with an IC_{50} value of 2–10 μM and a maximum inhibition of ≥70% (Fig. 4, *top*). The mean IC_{50} and maximum inhibition values measured in a sample of 25 of these cells are given in Table 1. For neurons >10 days *in vitro*, NMDA responses in 42% of the 36 cells examined were still blocked (IC_{50} = 2–10 μM); however, in these cells, only 28% of responses were blocked at ≥70% (Fig. 4, *bottom*). Indeed,

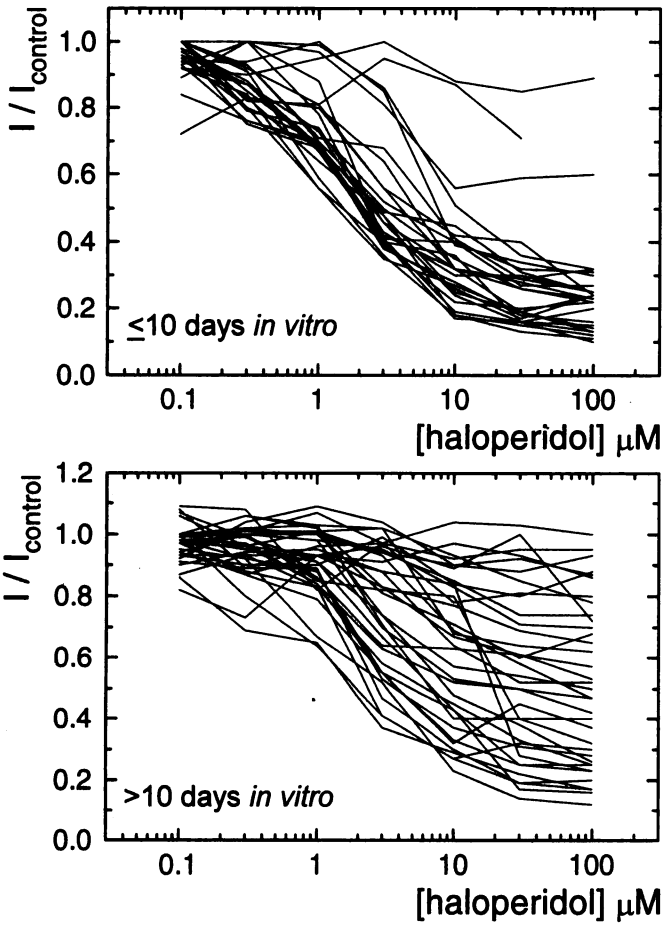

Fig. 4. Sensitivity of NMDA responses in cultured rat cortical neurons (embryonic day 16–17) to inhibition by haloperidol. *Top*, concentration-inhibition curves for haloperidol in neurons cultured for ≤10 days. *Bottom*, concentration-inhibition curves for haloperidol in neurons cultured for >10 days. Each *line graph* is from an individual neuron. Response amplitudes are expressed as a fraction of current elicited by 3 or 10 μM glycine and 100 μM NMDA. Current ranges and mean steady state responses were 25–1073 pA (244 ± 48 nA) for neurons ≤10 days *in vitro* (28 cells from five cultures) and 234-2288 nA (948 ± 77 pA) for neurons >10 days *in vitro* (36 cells from five cultures). Data are mean ± standard error.

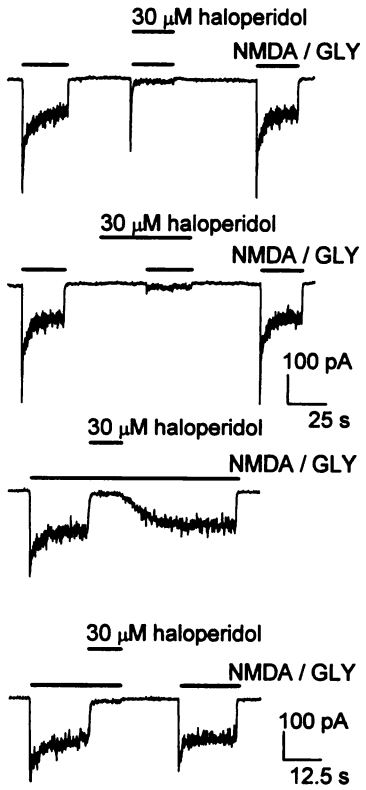

Fig. 5. Test for use dependence of NMDA receptor inhibition by haloperidol in cultured rat cortical neurons. *Top two traces*, inhibition induced by 30 μM haloperidol showing comparison between simultaneous application of antagonist and pretreatment with antagonist. Records were taken from the same cell; the second control was duplicated for the figure. *Bottom two traces*, noneffect of channel activation on washout of haloperidol inhibition. Records were taken from the same cell. *Scale bars* refer to top and bottom.

17% of the neurons had NMDA responses that were blocked <15% by 100 μM haloperidol (i.e., responses that were essentially insensitive to inhibition). For all subsequent experiments in which we investigated the mechanism of NMDA receptor inhibition, we used responses in neurons that showed high sensitivity to haloperidol. As seen in the oocyte experiments, haloperidol did not affect steady state neuronal AMPA responses (Table 1).

Mechanism of neuronal NMDA receptor antagonism. The mechanism of inhibition was investigated first by characterizing effects of a fixed concentration of haloperidol on concentration-response curves for glycine and glutamate. As described for NR1A/2B responses in oocytes, inhibition of neuronal NMDA responses by 5 μM haloperidol was not surmounted by raising concentrations of glycine or NMDA (not shown). Unlike NR1A/2B, inhibition was associated with a 2.9-fold decrease in apparent glycine affinity ($p < 0.01$) and a 50% increase in apparent affinity for NMDA that was not statistically significant ($0.3 < p < 0.5$) (Table 2).

Voltage dependence of inhibition was tested by comparing the levels of block induced by 3 μM haloperidol at two holding potentials: −60 mV and +50 mV. The fractional response was 0.59 ± 0.07 at −60 mV and 0.58 ± 0.06 at +50 mV (five experiments). These experiments indicated that a difference of 110 mV and reversal of the current had no effect on the potency of haloperidol inhibition ($p > 0.5$).

Use dependence of inhibition was assessed by testing whether preincubation and receptor activation had any effect on the onset and wash of antagonism, respectively (Fig. 5). Coapplication of agonists and 30 μM haloperidol resulted in a brief spike of current that decayed to the level of steady state inhibition (Fig. 5, *top two traces*). The time course of this decay reflected the combination of desensitization and binding of haloperidol. After preincubation in 30 μM haloperidol, the spike of current was greatly reduced or abolished, indicating that haloperidol was able to interact with the receptor before channel activation. The rate of washout of 30 μM haloperidol inhibition also seemed to be independent of agonist, indicating that channel activation is not necessary for washout of the blocker (Fig. 5, *bottom two traces*). Experiments in oocytes indicated that inhibition of NR1A/2B receptors by 30 μM haloperidol had similar properties. However, when using a 10-fold-lower concentration of haloperidol, the situation was more complex. In these experiments, the potency and onset of inhibition both seemed to be affected by channel activation (not shown).

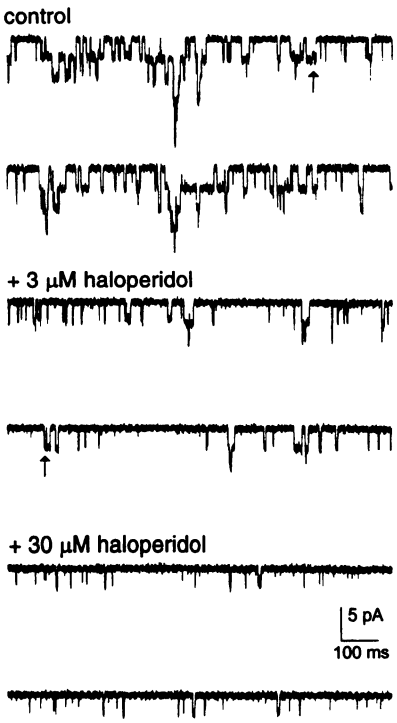

Fig. 6. Sample single-channel records illustrating inhibition of neuronal NMDA receptors by haloperidol. *Top*, single-channel activity under control conditions (0.5 μM glycine and 4 μM NMDA). *Middle*, the same patch with 3 μM haloperidol. *Bottom*, the same patch with 30 μM haloperidol. Single channels were recorded in outside-out patches excised from rat cortical neurons cultured for <10 days. *Arrows*, possible subconductance states.

TABLE 3

Inhibition of NMDA receptors by haloperidol measured at the single-channel level in excised outside-out patches from rat cortical neurons (5–10 days *in vitro*)

NMDA channels were activated by 0.5 μM glycine and 4 μM NMDA. Data are mean ± standard error.

	Control (n=11)	Haloperidol 3 μM (n=5)	Haloperidol 30 μM (n=8)
Amplitude (pA)	2.9 ± 0.04	2.8 ± 0.1	2.7 ± 0.1
Open time (msec)	5.0 ± 0.2	4.4 ± 0.3	3.0 ± 0.2
Open probability	0.043 ± 0.006	0.016 ± 0.006	0.007 ± 0.002

Actions on single-channel NMDA currents in cortical neurons. To further investigate the mechanism of haloperidol inhibition, we studied effects of the drug on NMDA-activated single-channel currents in outside-out membrane patches excised from the cultured cortical neurons. At a holding potential of −60 mV, application of NMDA and glycine activated well-resolved large conductance openings (Fig. 6, *top traces*). Coapplication of 3 μM haloperidol caused a substantial reduction in the number of channel openings (Fig. 6, *middle traces*). The effect was readily reversible. Increasing the haloperidol concentration up to 30 μM lead to an additional drop in the number of openings (Fig. 6, *bottom traces*). In multichannel patches, the mean open probability was decreased in a concentration-dependent manner by haloperidol (Table 3). There was good correlation between antagonism of single-channel activity and inhibition of the whole-cell current; 3 μM haloperidol reduced open probability to 37% of control, and 30 μM haloperidol reduced open probability to 15% of control.

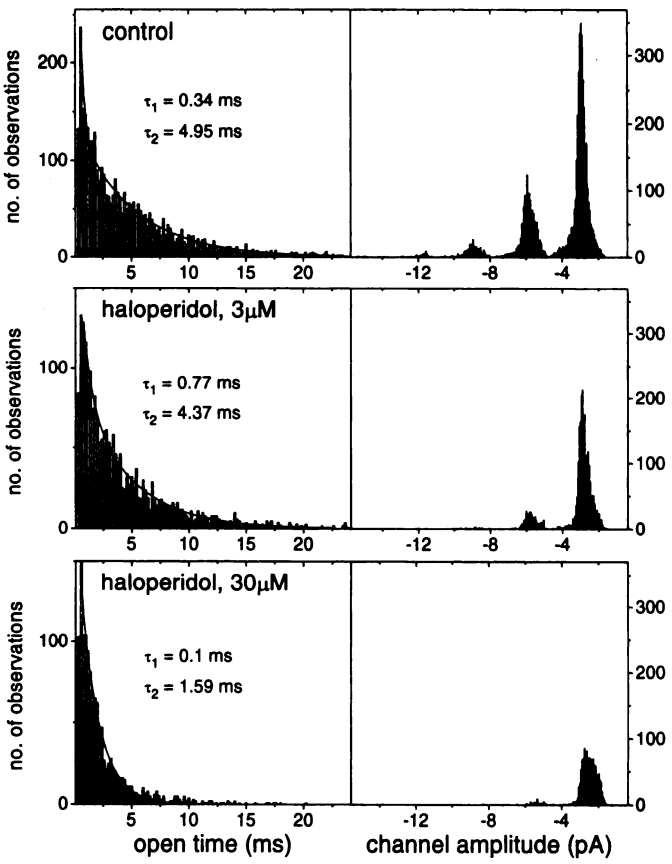

Fig. 7. Sample single-channel open-time and channel-amplitude histograms. Histograms were taken from the same patch under control conditions (0.5 μM glycine and 4 μM NMDA) and sequentially with 3 μM and then 30 μM haloperidol. The patch is the same as that used for the sample records in Fig. 6. *Smooth curves*, in each case, open-time distributions were best fit by the sum of two exponentials.

Amplitude histograms for one sample experiment are shown in Fig. 7 (same patch as Fig. 6). In this patch, multiple channels were active, and four separate peaks are seen in the control histogram. As previously reported (30), we observed subconductance states for NMDA-activated channels (e.g., Fig. 6, *arrows*). In the current study, we dealt only with the main conductance level; this was 48 ± 0.6 pS (five experiments), as calculated from the slope of the single-channel current/voltage curve (not shown). Haloperidol caused a slight, but statistically significant, reduction in single-channel amplitude ($p < 0.01$) (Table 3).

Haloperidol also had an effect on the open time of NMDA channels. Sample data for level 1 opening in a multichannel patch are shown in Fig. 7. Open-time histograms were best fit with the sum of two exponentials, both under control conditions and in the presence of haloperidol. We did not analyze the data in terms of multiple open states or bursting properties. Rather, we calculated an overall estimate of mean channel open time according to the approach proposed by Fenwick *et al.* (26) (see Materials and Methods). In this analysis, the mean open time was reduced 12% by 3 μM haloperidol and 40% by 30 μM haloperidol ($p < 0.001$) (Table 3).

Discussion

NR2B-selective inhibition of cloned NMDA receptors. A previous study reported that haloperidol inhibits NMDA-induced membrane current responses in cultured rat hippocampal neurons (19); the mechanism of inhibition seemed to involve partial agonism at NMDA receptor glycine sites. The current experiments show that haloperidol antagonizes cloned rat brain NMDA receptors expressed in *X. laevis* oocytes. The most striking feature of this inhibition is pronounced selectivity for NR1A/2B subunit combinations. Inhibition of NR1A/2B receptors by haloperidol is insurmountable with respect to glycine and glutamate and is incomplete. Incomplete antagonism often implies partial agonist activity. In this case, however, haloperidol induces little or no receptor activation when applied alone or when coapplied with either glycine or glutamate. These results indicate that inhibition of NR1A/2B receptors is due to interaction at a site that is distinct from coagonist binding sites. In particular, haloperidol is not a partial agonist for the glycine site. Potency of inhibition is independent of membrane voltage and onset, and wash of inhibition does not show simple use dependence. These two points argue that antagonism is not at the phencyclidine site (27, 31) or at inhibitory polyamine sites (32), both of which are located in the channel pore. Collectively, our results suggest that inhibition of NR1A/2B receptors by haloperidol is mediated by an allosteric modulatory site located on the extracellular surface of the receptor and that the integrity of this site is dependent on NR2B subunits. Details of haloperidol binding kinetics and allosteric interactions with agonist-binding sites will require further studies with systems more amenable to fast drug application techniques.

Effect of NR1 splice variants on haloperidol sensitivity. For NR2B subunit combinations, sensitivity to haloperidol is in large part unaffected by a change of the NR1 isoform from NR1A to either NR1B or NR1E. This implies that the amino-terminal insert (N1/exon 5), which is absent in NR1A and NR1e and present in NR1B, does not play a critical role in haloperidol binding or in transduction of allosteric inhibition (7, 21). Similarly, the two carboxyl-terminal splices (C1 and C2, involving exons 21 and 22), which are present in NR1A and NR1B but absent in NR1E, do not affect haloperidol inhibition. We cannot rule out the possibility that one of the isoforms may confer sensitivity to receptors containing NR2A, NR2C, or NR2D or that an untested splice combination might yet alter inhibition of NR1/2B. Nevertheless, these scenarios seem unlikely. Our results argue that the modifications to NR1 structure conferred by RNA splicing are not major determinants of haloperidol sensitivity.

Potentiation of NR1A/2A receptors. The potentiating effects on NR1A/2A receptors were seen only at high concentrations of haloperidol and were not present in all oocytes. Investigation of the mechanism of this effect and why there was variability among oocytes was beyond the scope of the current study. Still, it is worth noting that under saturating concentrations of agonist, the subtype-selectivity profile for haloperidol-induced potentiation is different from that of polyamines, which selectively potentiate NR1/2B receptors (33), or pregnenolone sulfate, which is a nonselective modulator.[2] We suspect that the NR2A-dependent potentiating effect may be related to the haloperidol-induced increases in NMDA responses that have been reported in cultured hippocampal neurons (19) and that were apparent in some of our own neuronal recordings.

Inhibition of neuronal NMDA receptors. For embryonic day 16–17 cortical neurons cultured for ≤10 days, NMDA receptors are, for the most part, sensitive to inhibition by haloperidol. Inhibition shares nearly all of the properties described for NR1A/2B receptors expressed in oocytes and is consistent with a similar mechanism of action. Potency of inhibition is comparable to that reported previously for hippocampal neurons (19), but in the current experiments, we do not find evidence for partial agonism at the glycine site. Our results suggest that embryonic day 16–17 neurons maintained for ≤10-days *in vitro* express NMDA receptors comprised of NR1/2B subunit combinations. This is consistent with *in vitro* mRNA assays (34) and with *in situ* hybridization and immunoprecipitation studies (5, 6), all of which indicate that NR2B is the predominant NR2 subunit expressed in embryonic neonatal rat forebrain.

Embryonic day 16–17 neurons cultured for >10 days have NMDA responses with a broad range of sensitivity to haloperidol. The most striking change is that it becomes increasingly common to find cells in which haloperidol induces very limited levels of block. The change in sensitivity to haloperidol coincides with a developmental switching-on of NR2A subunit expression that has been described to occur both *in situ* (5, 6, 12, 13) and *in vitro* (34). In the older cultures, the simplest explanation for limited sensitivity to haloperidol is that these neurons have begun to express NR2A subunits.

Inhibition of NMDA receptors at the single-channel level. The single-channel recordings were designed to address two specific issues: (i) whether inhibition induced by haloperidol could be mechanistically distinguished from the previously characterized NR2B-selective antagonist ifenprodil (9, 35) and (ii) whether inhibition of NMDA receptors by haloperidol could be mediated indirectly by a diffusible intracellular messenger molecule. Recent studies claim that haloperidol inhibits NMDA receptor function by interaction with σ receptors and an undefined inhibitory second-messenger pathway (36).

The main conductance level of NMDA-activated single-channel currents was 48 pS, which is in good agreement with the values of 40–50 pS reported previously (29, 30, 35). Recombinant NR1A/2A and NR1A/2B receptors expressed in *X. laevis* oocytes have conductances of ~50 pS (37) and are not readily distinguished. In general agreement with earlier studies (30, 35), single-channel open times showed two modes of gating. We did not systematically analyze the multimode time distributions. The mean open time calculated from our multichannel patches was ~5 msec, which fits well within the range of 3–10 msec previously reported for the NMDA receptor (29–31, 35).

At the single-channel level, haloperidol causes a pronounced decrease in the frequency of channel openings, a dose-dependent reduction in mean channel open time, and a slight decrease in channel amplitude. With respect to the first two effects, haloperidol is mechanistically similar to

[2] V. I. Ilyin, E. R. Whittemore, J. Guastella, E. Weber, and R. M. Woodward, unpublished observations.

ifenprodil (35). We suspect that the small decrease in channel amplitude (7% with 30 μM haloperidol) may simply be the result of inaccuracies in measurement as the number of events dropped and mean open duration shortened. Still, we cannot rule out the possibility that haloperidol promotes openings to a subconductance state or induces a negative shift in reversal potential. In the latter case, a shift of 5 mV would be sufficient to account for the reduction in channel amplitude. Like ifenprodil, haloperidol shows similarities with MK-801 and other blockers that use the "channel trap" mechanism (31, 35). Channel trap blockers decrease the open frequency and open duration time constants but do not typically affect channel conductance. Although they resemble channel trap blockers in single-channel recordings, haloperidol and ifenprodil have no related features at the level of whole-cell currents. In particular, antagonism shows neither voltage dependence nor simple use dependence (9, 35), whereas open channel blockers reduce whole-cell currents in a voltage- and agonist-dependent manner (31).

If haloperidol inhibits NMDA receptors via an indirect mechanism involving a cytosolic messenger molecule, then the excised-patch configuration should cause a significant reduction in potency. Our experiments indicate that there is no such effect. This strongly suggests that inhibition is not mediated through a second-messenger pathway (36). Viewed in conjunction with the whole-cell recordings, the single-channel data indicate that haloperidol inhibits NMDA-activated currents via a direct interaction at an allosteric site on the extracellular surface of the receptor.

Similarities with the atypical NMDA receptor antagonist ifenprodil. Inhibition of NMDA receptors by haloperidol has many features in common with the atypical NMDA receptor antagonist ifenprodil (9, 35): selectivity for NR1/2B receptors; incomplete, or two-component, block of NR1/2B receptor responses; insurmountable inhibition with respect to glutamate and glycine; absence of voltage dependence or simple use dependence; common actions on single-channel currents; and independence from the NR1 N1 insert. Although there remain minor differences between haloperidol and ifenprodil (9), overall, we suggest that the mechanisms of inhibition are related and that the two drugs interact at overlapping binding sites. Direct evidence supporting this view has been gained from binding studies in which haloperidol was found to displace [^{3}H]ifenprodil from mouse brain membranes at the same potency as it inhibits NMDA receptors.[3]

Haloperidol and ifenprodil are not closely related structurally but are both 1,4-disubstituted piperidines. If the two antagonists act at a common site on the NMDA receptor complex, it follows that this site will be amenable to a structurally diverse group of ligands. In particular, "hybrid" molecules should also be potent antagonists. This seems to have been borne out by the activity of CP-101,606, a recently described forebrain-selective NMDA receptor antagonist (38). Our results suggest that haloperidol could serve as a structural lead for developing novel subtype-selective NMDA receptor antagonists and thus therapeutically useful drugs for the treatment of ischemic stroke, epilepsy, and Parkinson's disease.

[3] L. L. Cougenhour and J. J. Corden, unpublished observations.

Relevance to the therapeutic effects of haloperidol. Haloperidol remains a commonly used neuroleptic that is effective in treating the positive symptoms of schizophrenia (17). The potency at which haloperidol interacts with D_2 dopamine receptors and σ sites is in the low nanomolar range (16, 17), which corresponds to the concentrations achieved in the cerebrospinal fluid of schizophrenic patients after a typical clinical dosage. Appreciable antagonism of NMDA receptors requires concentrations of >100 nM haloperidol, suggesting that inhibition of NMDA receptors is not relevant to antipsychotic efficacy. Interestingly, a recent report proposes that the antipsychotic effects of haloperidol may be due, conversely, to potent positive allosteric modulation of NMDA receptors (39). In this study, nanomolar concentrations of haloperidol were found to transiently augment excitatory synaptic field potentials in rat striatum and to increase [^{3}H]MK-801 binding to rat brain membranes. Higher concentrations of haloperidol were inhibitory in both assays, as would be predicted on the basis of the current experiments. We did not routinely test low (<30 nM) concentrations of haloperidol for effects on NMDA responses, particularly under nonsaturating agonist concentrations (39). Further studies will therefore be necessary to investigate whether haloperidol has any additional potent potentiating effects on NMDA receptor responses.

References

1. Hollmann, M., and S. Heinemann. Cloned glutamate receptors. *Annu. Rev. Neurosci.* **17**:31–108 (1994).
2. Moriyoshi, K., M. Masu, T. Ishii, R. Shigemoto, N. Mizuno, and S. Nakanishi. Molecular cloning and characterization of the rat NMDA receptor. *Nature (Lond.)* **354**:31–37 (1991).
3. Monyer, H., R. Sprengel, R. Schoepfer, A. Herb, M. Higuchi, H. Lomeli, N. Burnashev, B. Sakmann, and P. H. Seeburg. Heteromeric NMDA receptors: molecular and functional distinction of subtypes. *Science (Washington D. C.)* **256**:1217–1221 (1992).
4. Kutsuwada, T., N. Kashiwabuchi, H. Mori, K. Sakimua, E. Kushiya, K. Araki, H. Meguro, H. Masaki, T. Kumanihsi, M. Arakawa, and M. Mishina. Molecular diversity of the NMDA receptor channel. *Nature (Lond.)* **358**:36–41 (1992).
5. Sheng, M., J. Cummings, L. A. Roldan, Y. N. Jan, and L. Y. Jan. Changing subunit composition of heteromeric NMDA receptors during development of rat cortex. *Nature (Lond.)* **368**:144–147 (1994).
6. Monyer, H., N. Burnashev, D. J. Laurie, B. Sakmann, and P. H. Seeburg. Developmental and regional expression in the rat brain and functional properties of four NMDA receptors. *Neuron* **12**:529–540 (1994).
7. Zukin, R. S., and M. V. L. Bennett. Alternatively spliced isoforms of the NMDAR1 receptor subunit. *Trends Neurosci.* **18**:306–313 (1995).
8. Priestly, T., P. Laughton, J. Myers, B. Le Bourdelles, J. Kirby, and P. J. Whiting. Pharmacological properties of recombinant human *N*-methyl-D-aspartate receptors comprising NR1a/NR2A and NR1a/2B subunit assemblies expressed in permanently transfected mouse fibroblast cells. *Mol. Pharmacol.* **48**:841–848 (1995).
9. Williams, K. Ifenprodil discriminates subtypes of the *N*-methyl-D-aspartate receptor: selectivity and mechanisms at recombinant heteromeric receptors. *Mol. Pharmacol.* **44**:851–859 (1993).
10. Woodward, R. M., J. E. Huettner, J. Guastella, J. F. W. Keana, and E. Weber. *In vitro* pharmacology of ACEA-1021 and ACEA-1031: systemically active quinoxalinediones with high affinity and selectivity for *N*-methyl-D-aspartate receptor glycine sites. *Mol. Pharmacol.* **47**:568–581 (1995).
11. Ben-Ari, Y., E. Cherubini, and K. Krnjevic. Changes in voltage-dependence of NMDA currents during development. *Neurosci. Lett.* **94**:88–92 (1988).
12. Vicini, S., J. F. Wang, J. S. Poling, and D. R. Grayson. Functional and pharmacological differences between recombinant and native NMDA receptors. *Soc. Neurosci. Abstr.* **21**:86 (1995).
13. Williams, K., S. L. Russell, Y. M. Shen, and P. B. Molinoff. Developmental switch in the expression of NMDA receptors occurs *in vivo* and *in vitro*. *Neuron* **10**:267–278 (1993).
14. Choi, D. W., and S. M. Rothman. The role of glutamate neurotoxicity in hypoxic-ischemic neuronal death. *Annu. Rev. Neurosci.* **13**:171–182 (1990).
15. Muir, K. W., and K. R. Lees. Clinical experience with excitatory amino acid antagonist drugs. *Stroke* **26**:503–513 (1995).
16. Peroutka, S. J., and S. H. Snyder. Relationship of neuroleptic drug effects at brain dopamine, serotonin, α-adrenergic, and histamine receptors to clinical potency. *Am. J. Psychiatry* **137**:1518–1522 (1980).

17. Itzhak, Y., and I. Stein. *Sigma* binding sites in the brain: an emerging concept for multiple sites and their relevance to psychiatric disorders. *Life Sci.* **47**:1073–1081 (1990).
18. MacDonald, J. W., and M. V. Johnston. Pharmacology of NMDA-induced brain injury in an *in vivo* perinatal rat model. *Synapse* **6**:179–188 (1990).
19. Fletcher, E. J., and J. F. MacDonald. Haloperidol interacts with the strychnine-insensitive glycine site at the NMDA receptor in cultured mouse hippocampal neurones. *Eu. J. Pharmacol.* **235**:291–295 (1993).
20. Leeson, P. D. Glycine-site N-methyl-D-aspartate receptor antagonists, in *Drug Design for Neuroscience* (A. P. Kozikowski, ed.). Raven Press, New York, 339–381 (1993).
21. Sugihara, H., K. Moriyoshi, T. Ishii, M. Masu, and S. Nakanishi. Structures and properties of seven isoforms of the NMDA receptor generated by alternative splicing. *Biochem. Biophys. Res. Commun.* **185**:826–832 (1992).
22. Ilyin, V. I., J. Guastella, S. X. Cai, E. Weber, and R. M. Woodward. Subunit-specific inhibition of cloned NMDA receptors by haloperidol. *Soc. Neurosci. Abstr.* **20**:1143 (1994).
23. Whittemore, E. R., D. T. Loo, J. A. Watt, and C. W. Cotman. A detailed analysis of hydrogen peroxide-induced cell death in primary neuronal culture. *Neuroscience* **67**:921–932 (1995).
24. Hamill, O. P., Marty A., Neher E., Sakmann B., and F. J. Sigworth. Improved patch-clamp techniques for high-resolution current recording from cells and cell-free membrane patches. *Pflueg. Arch. Eur. J. Physiol.* **391**:85–100 (1981).
25. Colquhoun, D., and F. J. Sigworth. Fitting and statistical analysis of single-channel records, in *Single-Channel Recording* (B. Sakmann and E. Neher, eds.). Plenum Press, New York/London, 483–587 (1995).
26. Fenwick, E. M., Marty, A., and E. Neher. Sodium and calcium channels in bovine chromaffin cells. *J. Physiol. (Lond.)* **331**:599–635 (1982).
27. MacDonald, J. F., M. C. Bartlett, I. Mody, P. Paphapill, J. N. Reynolds, M. W. Slater, J. H. Schneiderman, and P. S. Pennefather. Actions of ketamine, phencyclidine and MK-801 on NMDA receptor currents in cultured mouse hippocampal neurones. *J. Physiol. (Lond.)* **432**:483–508 (1991).
28. Arellano, R. O., R. M. Woodward, and R. Miledi. A monovalent cationic conductance that is blocked by extracellular divalent cations in *Xenopus* oocytes. *J. Physiol. (Lond.)* **484**:3:593–604 (1995).
29. Ascher, P., P. Bregestovski, and L. Nowak. N-Methyl-D-aspartate-activated channels of mouse central neurones in magnesium-free solutions. *J. Physiol. (Lond.)* **399**:207–226 (1988).
30. Jahr, C. E., and C. F. Stevens. Glutamate activates multiple single channel conductances in hippocampal neurons. *Nature (Lond.)* **325**:522–525 (1987).
31. Huettner, J. E., and B. P. Bean. Block of N-methyl-D-aspartate-activated current by the anticonvulsant MK-801: selective binding to open channels. *Proc. Natl. Acad. Sci. USA* **85**:1307–1311 (1988).
32. Benveniste, M., and M. L. Mayer. Multiple effects of spermine on N-methyl-D-aspartate receptor responses of rat cultured hippocampal neurons. *J. Physiol. (Lond.)* **464**:131–163 (1993)
33. Williams, K. Mechanisms influencing stimulatory effects of spermine at recombinant *N*-methyl-D-aspartate receptors. *Mol. Pharmacol.* **46**:161–168 (1994).
34. Zhong, J., S. L. Russel, D. B. Prichett, P. B. Molinoff, and K. Williams. Expression of messenger RNAs encoding subunits of the *N*-methyl-D-aspartate receptor in cultured cortical neurons. *Mol. Pharmacol.* **45**:846–853 (1994).
35. Legendre, P., and G. L. Westbrook. Ifenprodil blocks *N*-methyl-D-aspartate receptors by a two-component mechanism. *Mol. Pharmacol.* **40**:289–298 (1991).
36. Yamamoto, H., Y. Yamamoto, N. Sagi, V. Klenerova, K. Goji, N. Kawai, A. Baba, E. Takamori, and T. Moroji. *Sigma* ligands indirectly modulate the NMDA receptor-ion channel complex on intact neuronal cells via σ1 site. *J. Neurosci.* **15**:731–736 (1995).
37. Stern, P., P. Behe, R. Schoepfer, and D. Colquhoun. Single-channel conductances of NMDA receptors expressed from cloned cDNAs: comparison with native receptors. *Proc. R. Soc. Lond. B Biol. Sci.* **250**:271–277 (1992).
38. Chenard, B. L., J. Bordner, T. W. Butler, L. K. Chambers, M. A. Collins, D. L. De Costa, M. F. Ducat, M. L. Dumont, C. B. Fox, E. E. Mena, F. S. Meniti, J. Nielsen, M. J. Pagnozzi, K. E. G. Richter, R. T. Ronau, I A. Shalaby, J. Z. Stemple, and W. F. White. (1S,2S)-1-(4-Hydroxyphenyl)-2-(4-hydroxy-4-phenylpiperidino)-1-propanol: a potent new neuroprotectant which blocks N-methyl-D-aspartate responses. *J. Med. Chem.* **38**:3138–3145 (1995).
39. Banerjee, S. P., L. G. Zuck, E. Yablonsky-Alter, and T. I. Lidsky. Glutamate agonist activity: implications for antipsychotic drug actions and schizophrenia. *Neuroreport* **6**:2500–2504 (1995).

Send reprint requests to: Dr. R. M. Woodward, Acea Pharmaceuticals Inc., 1003 Health Sciences Road West, Irvine, CA 92612.